Supplementary Information for

# Chitosan-based grafted cationic magnetic material to remove emulsified oil in wastewater: Performance and mechanism

Sicong Du, Chuang Liu, Peng Cheng, Wenyan Liang*

Beijing Key Lab for Source Control Technology of Water Pollution; Engineering Research Center for Water Pollution Source Control & Eco-remediation; College of Environmental Science and Engineering, Beijing Forestry University, Beijing 100083, China

**The supplementary information contains:**

**Materials and methods**



**Results and discussion**

## Materials and methods

### S1. Schematic diagram of particle image velocimetry setup

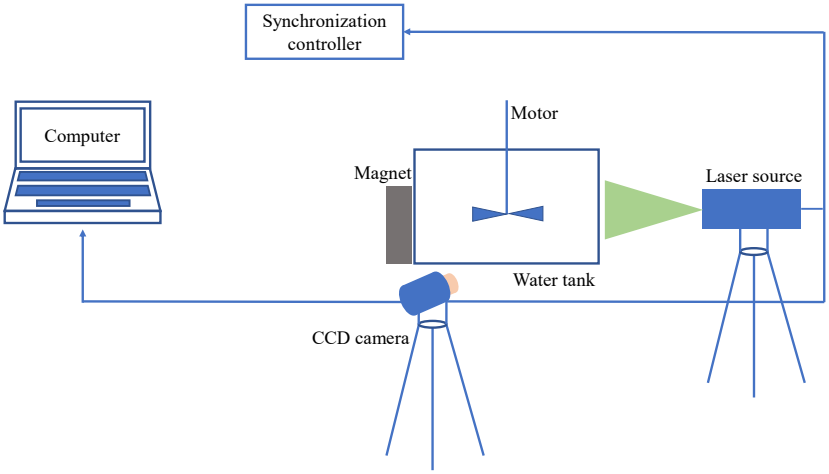


**Figure S1** Schematic diagram of Particle Image Velocimetry setup.

### S2. DLVO, EDLVO, and MDLVO theory

The magnetic flocculation mechanism of emulsified oil droplets and FS@CTS-P(AM-DMC) was analyzed using the modified DLVO theory. For the classical DLVO model, the total interaction energy ($U_{DLVO}$) between surfaces is the sum of the van der Waals interaction energy ($U_{vdw}$) and the electrostatic interaction energy ($U_{EL}$). In the extended DLVO (EDLVO) theory, the total interaction energy includes the van der Waals interaction energy ($U_{vdw}$), the electrostatic interaction energy ($U_{EL}$), and the Lewis acid-base interaction energy ($U_{AB}$). In the magnetically modified EDLVO theory, the total interaction energy needs to consider the magnetic interaction energy (UM). The total interaction energy between interacting particles can be calculated using the following Equations:

$$U_{DLVO}(h) = U_{vdw}(h) + U_{EL}(h) \tag{S1}$$

$$U_{EDLVO}(h) = U_{DLVO}(h) + U_{AB}(h) \tag{S2}$$

$$U_{MDLVO}(h) = U_{EDLVO}(h) + U_{MF}(h) \tag{S3}$$

The four types of interaction forces can be simulated by Equation S4-S7:

$$U_{vdw}(h) = -\frac{AR_1R_2}{6h(R_1+R_2)} \tag{S4}$$

$$U_{EL}(h) = \frac{\pi\varepsilon R_1R_2\left(\psi_1^2+\psi_2^2\right)}{(R_1+R_2)}\left[\frac{2\psi_1\psi_2}{\psi_1^2+\psi_2^2}\ln\frac{1+\exp(-kh)}{1-\exp(-kh)}+\ln\{1-\exp(-2kh)\}\right] \tag{S5}$$

$$U_{AB}(h) = 2\pi\frac{R_1R_2}{R_1+R_2}\lambda\Delta G_{h_0}^{AB}[\exp(h_0-h)/\lambda] \tag{S6}$$

$$U_M(h) = -\frac{8\pi\mu_0M_S^2R^3}{9\left(\frac{h}{R}+2\right)^3} \tag{S7}$$

All the parameters used in the above equations were detailly summarized in Tables S1-S3:

**Table S1** Parameters used in DLVO, EDLVO and MDLVO equations.

| | |
|---|---|
| $R$ | The radius of FS@CTS-P(AM-DMC) and emulsified oil droplet. |
| $A_{132}$ | The effective Hamaker constant (J) for particles (1) interacting with particles (2) in the aqueous medium (3). |
| $h_0$ | The shortest distance between the particles, 0.157 nm [1]. |
| $h$ | The separation distance between the two interacting particles (nm). |
| $\kappa$ | The inverse of the Debye length ($m^{-1}$). |
| $\lambda$ | The correlation length of molecules in the liquid medium, 0.6 nm. |
| $\varepsilon$ | The dielectric constant of the solution, ($80\times8.854\times10^{-12}$ $C^2/J/m$ for aqueous). |
| $\psi$ | The zeta potential of colloidal particles (mV). |
| $N_A$ | Avogadro's number, $6.02\times10^{23}$ $mol^{-1}$. |
| $e$ | Elementary charge, $1.602\times 10^{-19}$ C. |
| $T$ | Absolute temperature, 298 K. |
| $K$ | Boltzmann constant, $1.38\times 10^{-23}$ J/K. |
| $I$ | Ionic strength |
| $\mu_0$ | The magnetic permeability of vacuum ($\mu_0 = 1.26 \times 10^{-6}$ $Tm \cdot A^{-1}$). |
| $M$s | The magnetization of the particles, $A\cdot m^{-1}$. |

**Table S2** Characteristics of FS@CTS-P(AM-DMC) and emulsified oil droplet.

| Characteristics | FS@CTS-P(AM-DMC) | emulsified oil droplet |
|---|---|---|
| Particle radius (nm) | 10300 | 1585 |
| Magnetic saturation (kA/m) | 53.81 | - |

**Table S3** Surface tension and components of liquid ($mJ/m^2$).

| Liquid | $\gamma_L$ | $\gamma_L^{LW}(\gamma_L^d)$ | $\gamma_L^{AB}(\gamma_L^P)$ | $\gamma_L^+$ | $\gamma_L^-$ |
|---|---|---|---|---|---|
| Water | 72.8 | 21.8 | 51.0 | 25.5 | 25.5 |
| Diiodomethane | 58.0 | 39.0 | 19.0 | 2.28 | 39.6 |
| Formamide | 50.8 | 50.8 | 0 | 0 | 0 |

The contact angle (θ) of FS@CTS-P(AM-DMC) was measured using a contact angle measurement instrument (OCA20, Dataphysics, Germany). For emulsified oil whose surface tension components were not readily available, the pendant drop method was used to determine the surface tension components [2]. Then, according to the Extended Young's equation (Equation S8), the polar and apolar surface tensions were calculated, as summarized in Table S4 for contact angles and polar surface tension. The Hamaker constant was calculated

based on these surface tension results, as shown in Table S5.

$$\gamma_L(1+cos\theta) = 2(\gamma_B^{LW}\gamma_B^{LW})^{1/2} + 2(\gamma_B^{+}\gamma_B^{-})^{1/2} + 2(\gamma_B^{-}\gamma_B^{+})^{1/2} \quad \text{(S8)}$$

$$A = -12\pi h_0^2 \Delta G_{adh}^{LW} \quad \text{(S9)}$$

$$\Delta G_{adh}^{LW} = -2\gamma_{BL}^{LW} = -2 \times \left(\sqrt{\gamma_B^{LW}} - \sqrt{\gamma_L^{LW}}\right)^2 \quad \text{(S10)}$$

**Table S4** The contact angles for flocculants and the calculated surface tension energy components.

| Surface | Contact angles (°) | | | Surface tension (mJ/m²) | | |
|---|---|---|---|---|---|---|
| | Water | Formimide | Diiodomethane | $\gamma_i^{LW}$ | $\gamma_i^{+}$ | $\gamma_i^{-}$ |
| FS@CTS-P(AM-DMC) | 13.09 | 17.94 | 20.09 | 47.76 | 0.11 | 56.34 |
| emulsified oil droplet | - | - | - | 35.03 | 2.34 | 54.95 |

**Table S5** The Hamaker constants for the interacting emulsified oil droplets and flocculants.

| Surface | $A_{131}/A_{132}$ (J) | |
|---|---|---|
| | FS@CTS-P(AM-DMC) | emulsified oil droplet |
| FS@CTS-P(AM-DMC) | $9.34\times10^{-21}$ | $5.21\times10^{-21}$ |
| emulsified oil droplet | $5.21\times10^{-21}$ | $2.9\times10^{-21}$ |

## Results and discussion

### S3. The effect of initial oil concentration.

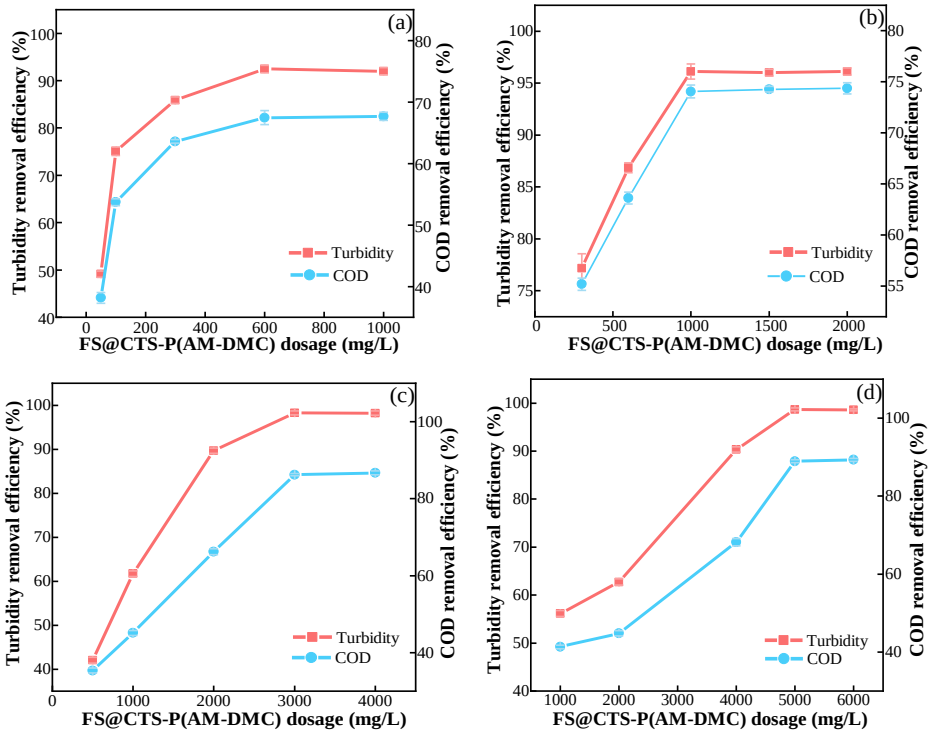


**Figure S2** Effect of initial oil concentration on removal efficiency using FS@CTS-P(AM-DMC), (a)200 mg/L, (b)500 mg/L, (c)2000 mg/L, (d)3000 mg/L. Stirring speed = 400 r/min. Stirring time = 10 min. Settling time = 3 min.

**S4. The comparison of the reported removal efficiency of different magnetic flocculants for emulsified oily wastewater.**

**Table S6** Comparison of the reported removal efficiency of different magnetic flocculants for emulsified oily wastewater.

| Materials | Water quality parameters of raw water | Removal efficiency | Dosage | Reference |
|---|---|---|---|---|
| PAM-g-MagCell | Turbidity：492 NTU<br>COD：12553 mg/L | Turbidity removal：88.62 %<br>COD removal：53.23 % | 1500 mg/L | [3] |
| $Fe_3O_4$@OA | oil concentration：0.3 wt% | demulsification efficiency (ED):97% | 3 g/L | [4] |
| FS-MC | oil concentration：10.3-14.6 mg/L<br>Turbidity：26.1-37.6 NTU<br>COD：40.6-90.3 mg/L | Oil removal:95.79 %<br>Turbidity removal：87.85 %<br>COD removal：66.67 % | 4-6 ml/L | [5] |
| FS-MC | oil concentration：130±20 mg/L | Oil removal:93 % | 2 mg/L | [6] |
| $Fe_3O_4$@$SiO_2$@Epoxy | oil concentration：7.4 g/L | Oil removal:92.3 % | 2.5 g/L | [7] |
| PVP- coated NPs | oil concentration：150±5 mg/L | Oil removal: 99 % | 4.4ppm-70.2ppm | [8] |
| PVP-coated $Fe_3O_4$ MNPs | oil concentration：2700 mg/L | Oil removal: 90-99 % | 1-2 g/L | [9] |
| EP@APTES-$Fe_3O_4$ | oil concentration：1.0 wt% | ED:95% | 500 mg/L | [10] |
| QC-grafted MNPs | oil concentration：0.2 wt%% | ED:90-100 % | 0–1.8 g/L | [11] |
| $Fe_3O_4$@OA | oil concentration：10 g/L | Oil removal: 98% | 30 g/L | [12] |
| $Fe_3O_4$@OA | oil concentration：3.3 g/L | Oil removal: 97% | 100 g/L | [13] |
| FS@CTS-P(AM-DMC) | oil concentration：1000 mg/L<br>Turbidity：950 ± 50 NTU<br>COD：1150 ± 50 mg/L | Turbidity removal：96.4 %<br>COD removal：74.5 % | 2 g/L | this study |

**S5. The effect of magnetic field strength.**

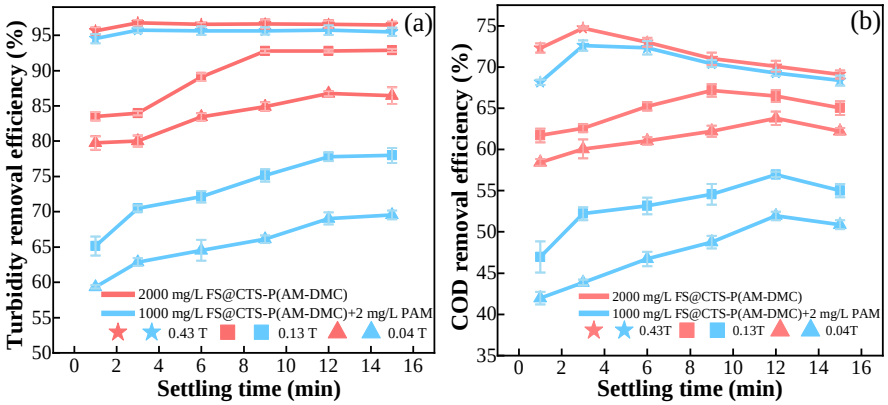


**Figure S3** Effect of magnetic field strength on removal (a) turbidity and (b) COD efficiency. Stirring speed = 400 r/min. Stirring time = 10 min.

**S6. The evolution of Floc size formed by FS@CTS-P(AM-DMC) under different dosing strategies and pH levels.**

**Table S7** The properties of flocs under different dosing modes and pH levels.

| Dosing mode | pH | Rapid stirring growth rate (μm min$^{-1}$) | Magnetic separation growth rate (μm min$^{-1}$) | Strength factor (%) | Recovery factor (%) |
|---|---|---|---|---|---|
| 2000 mg/L FS@CTS-P(AM-DMC) | 5.0 | 12.30 | 14.75 | 75.10 | 80.53 |
| | 7.0 | 11.88 | 14.42 | 69.27 | 76.79 |
| | 9.0 | 9.78 | 14.14 | 65.08 | 73.14 |
| 1000 mg/L FS@CTS-P(AM-DMC) + PAM 2 mg/L | 5.0 | 15.63 | 43.14 | 47.41 | 57.88 |
| | 7.0 | 14.86 | 44.64 | 46.73 | 51.47 |
| | 9.0 | 14.32 | 44.86 | 44.52 | 52.22 |

**S7. The microscopic images of FS@CTS-P(AM-DMC)-emulsified oil flocs during rapid stirring process.**

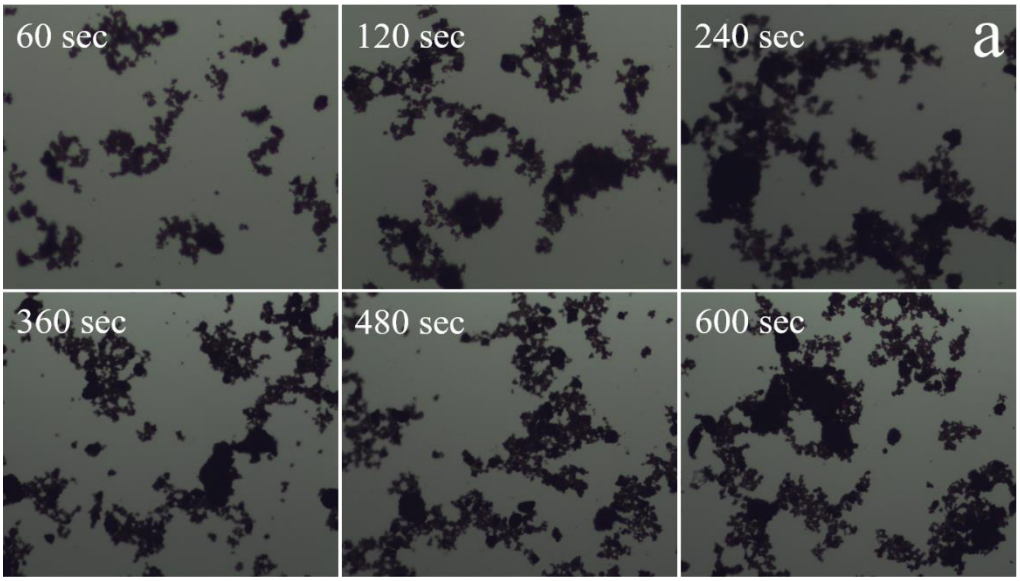

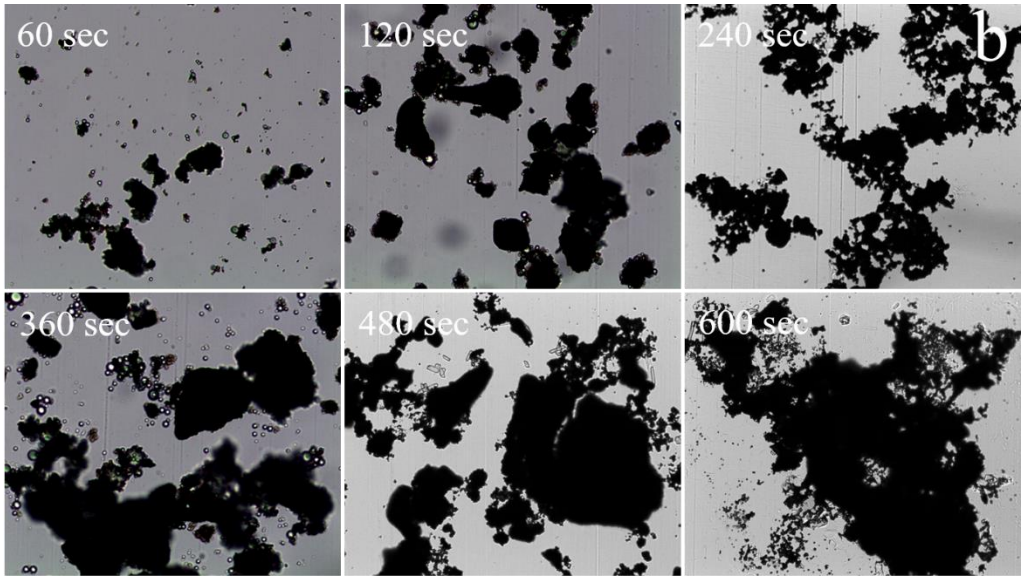


**Figure S4** The microscopic images of FS@CTS-P(AM-DMC)-emulsified oil flocs during rapid stirring process for two dosing modes, (a) 2000 mg/L FS@CTS-P(AM-DMC), (b) 1000 mg/L FS@CTS-P(AM-DMC) + 2 mg/L PAM. pH = 7.0. Stirring speed = 400 r/min. Stirring time = 10 min.

**S8. The microscopic images of FS@CTS-P(AM-DMC)-emulsified oil flocs during magnetic separation process.**

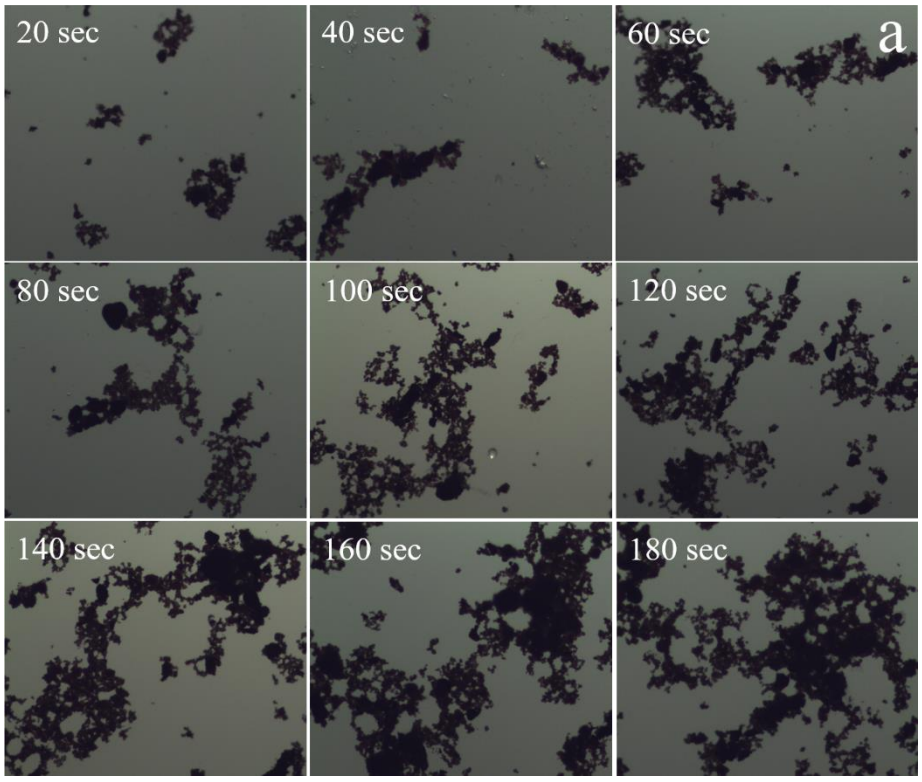

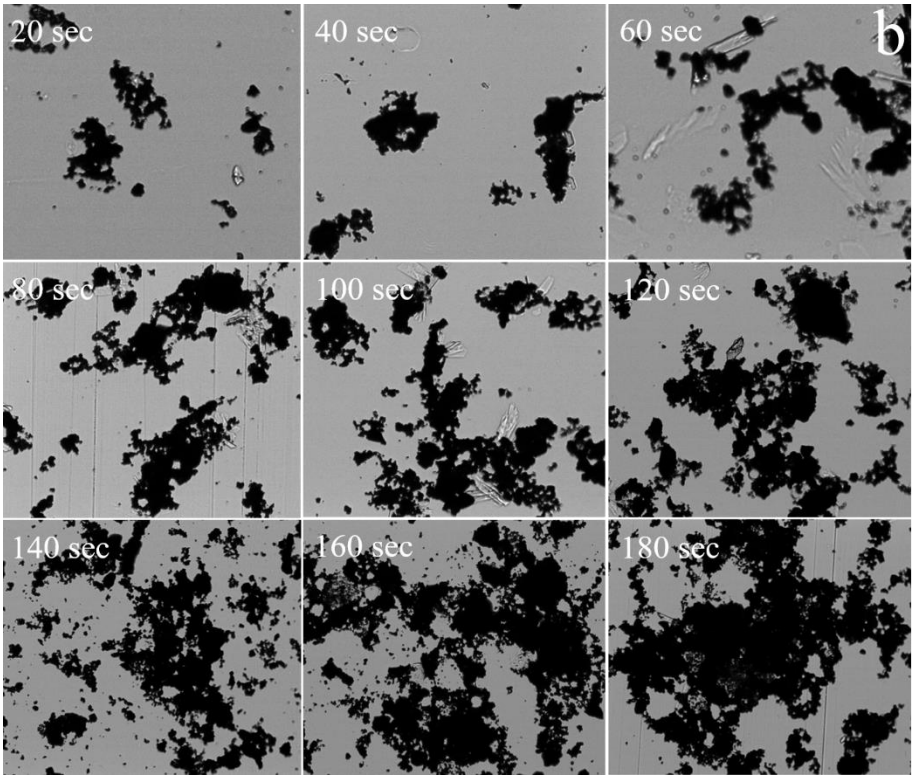


**Figure S5** The microscopic images of FS@CTS-P(AM-DMC)-emulsified oil flocs during magnetic separation process for two dosing modes, (a) 2000 mg/L FS@CTS-P(AM-DMC), (b) 1000 mg/L FS@CTS-P(AM-DMC) + 2 mg/L PAM. pH = 7.0. Stirring speed = 400 r/min. Settling time = 3 min.

**S9. The DLVO analysis between emulsified oil droplet and emulsified oil droplet.**

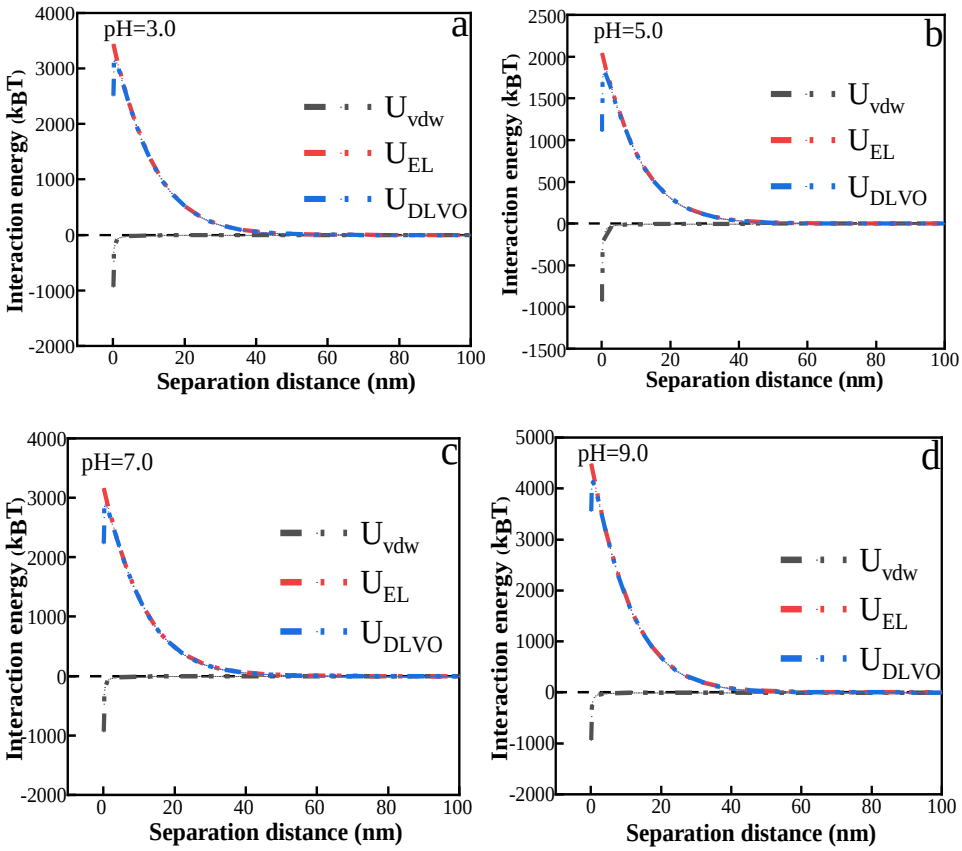

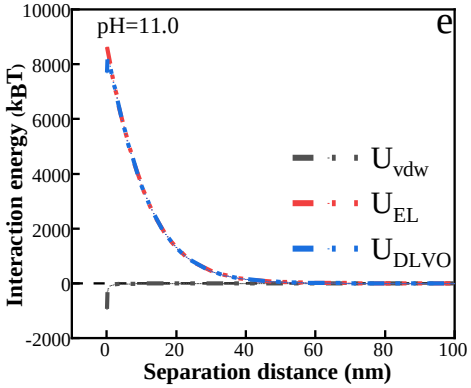


**Figure S6** Interaction energy versus interaction distance between different interacting entities: oil droplet and emulsified oil droplet (a-e).

**S10. The DLVO analysis between emulsified oil droplet and FS@CTS-P(AM-DMC).**

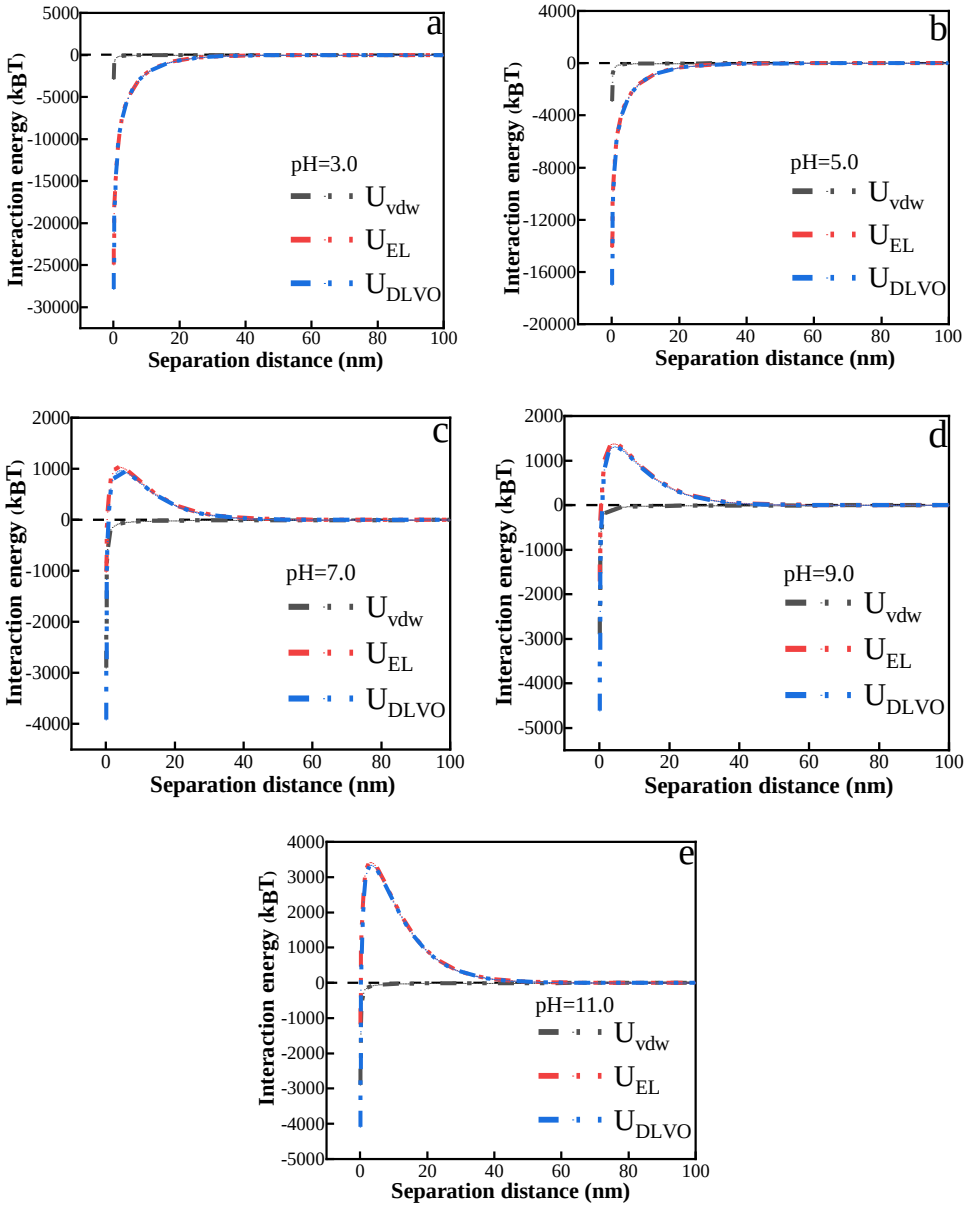


**Figure S7** Interaction energy versus interaction distance between different interacting entities: oil droplet

and FS@CTS-P(AM-DMC) (a-e).

**S11. The DLVO analysis between FS@CTS-P(AM-DMC) and FS@CTS-P(AM-DMC).**

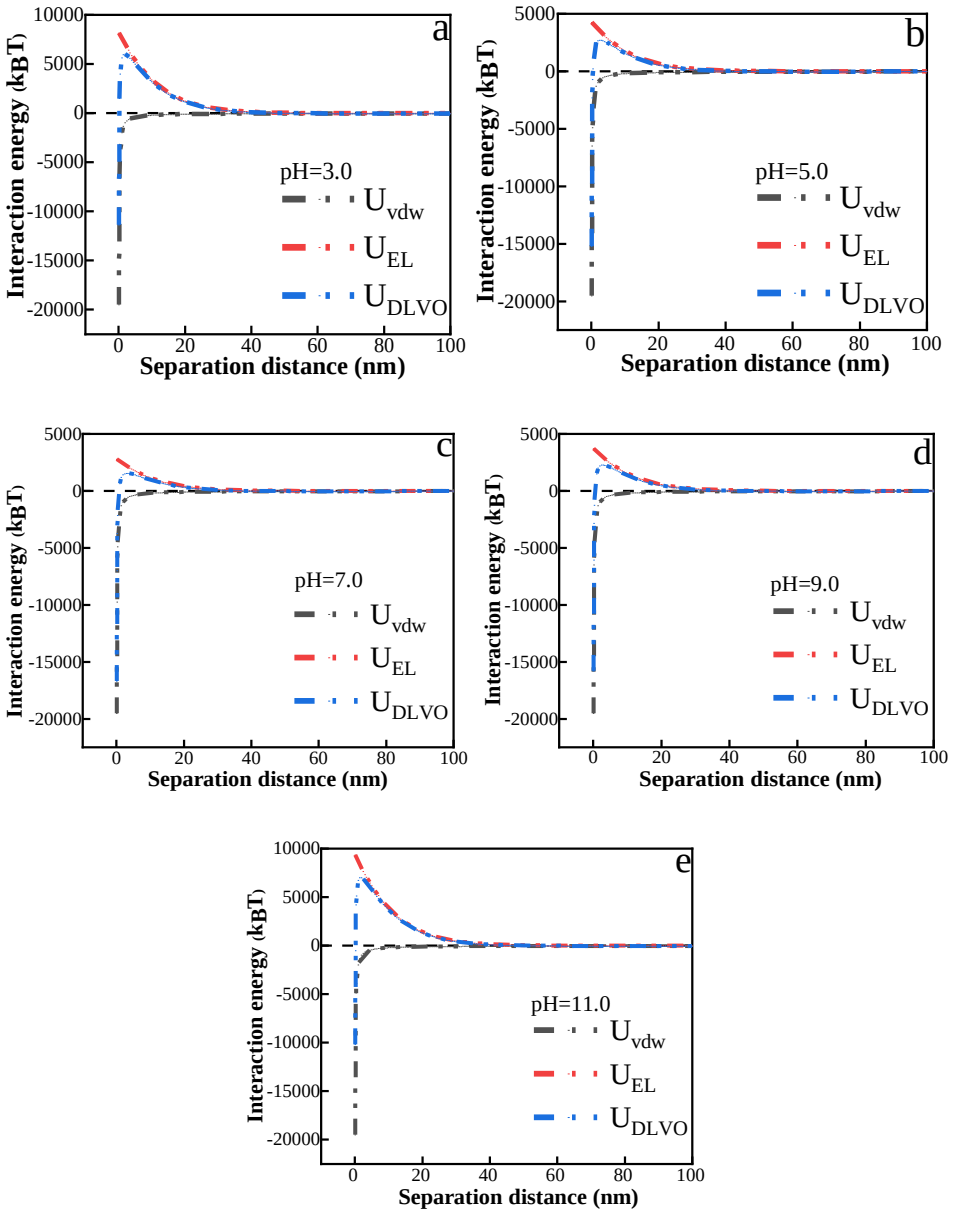


**Figure S8** Interaction energy versus interaction distance between different interacting entities: FS@CTS-P(AM-DMC) and FS@CTS-P(AM-DMC) (a-e).

## S12. The EDLVO analysis

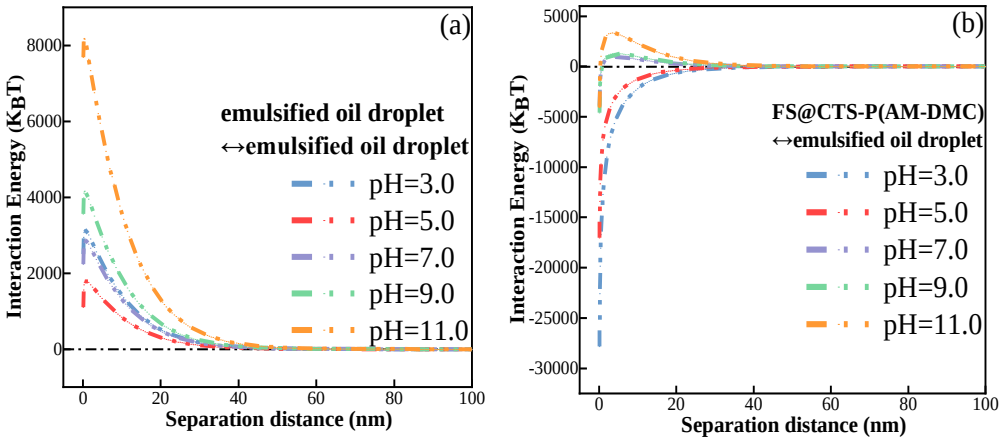


**Figure S9** Interaction energy of EDLVO between (a) oil emulsified droplet and oil emulsified droplet, (b) FS@CTS-P(AM-DMC) and oil emulsified droplet.

## References


1. Xu, J.; Yu, H.Q.; Li, X.Y. Probing the contribution of extracellular polymeric substance fractions to activated-sludge bioflocculation using particle image velocimetry in combination with extended DLVO analysis. *Chem. Eng. J.* **2016**, *303*, 627-635, doi:10.1016/j.cej.2016.06.042.
2. Tanudjaja, H.J.; Chew, J.W. Assessment of oil fouling by oil-membrane interaction energy analysis. *Journal of Membrane Science* **2018**, *560*, 21-29, doi:10.1016/j.memsci.2018.05.008.
3. Mohamed Noor, M.H.; Ngadi, N.; Mohammed Inuwa, I.; Opotu, L.A.; Mohd Nawawi, M.G. Synthesis and application of polyacrylamide grafted magnetic cellulose flocculant for palm oil wastewater treatment. *Journal of Environmental Chemical Engineering* **2020**, *8*, 104014, doi:10.1016/j.jece.2020.104014.
4. Hu, L.; Gao, S.; Ding, X.; Wang, D.; Jiang, J.; Jin, J.; Jiang, L. Photothermo-Responsive Single-Walled Carbon Nanotube-Based Ultrathin Membranes for On/Off Switchable Separation of Oil-in-Water Nanoemulsions. *ACS nano* **2015**, *9*, 4835-4842, doi:10.1021/nn5062854.
5. Ma, J.; Wu, G.; Zhang, R.; Xia, W.; Nie, Y.; Kong, Y.; Jia, B.; Li, S. Emulsified oil removal from steel rolling oily wastewater by using magnetic chitosan-based flocculants: Flocculation performance, mechanism, and the effect of hydrophobic monomer ratio. *Separation and Purification Technology* **2023**, *304*, 122329, doi:10.1016/j.seppur.2022.122329.
6. Ma, J.; Fu, X.; Xia, W.; Zhang, R.; Fu, K.; Wu, G.; Jia, B.; Li, S.; Li, J. Removal of emulsified oil from water by using recyclable chitosan based covalently bonded composite magnetic flocculant: Performance and mechanism. *J Hazard Mater* **2021**, *419*, 126529, doi:10.1016/j.jhazmat.2021.126529.
7. Duan, M.; Xu, Z.; Zhang, Y.; Fang, S.; Song, X.; Xiong, Y. Core-shell composite nanoparticles with magnetic and temperature dual stimuli-responsive properties for removing emulsified oil. *Advanced Powder Technology* **2017**, *28*, 1291-1297, doi:10.1016/j.apt.2017.02.017.
8. Mirshahghassemi, S.; Lead, J.R. Oil Recovery from Water under Environmentally Relevant Conditions Using Magnetic Nanoparticles. *Environ Sci Technol* **2015**, *49*, 11729-11736, doi:10.1021/acs.est.5b02687.
9. Shao; Li; Lü; Qi; Zhang; Zhao. Removal of Emulsified Oil from Aqueous Environment by Using Polyvinylpyrrolidone-Coated Magnetic Nanoparticles. *Water* **2019**, *11*, 1993,

doi:10.3390/w11101993.

10. Xu, H.; Jia, W.; Ren, S.; Wang, J. Novel and recyclable demulsifier of expanded perlite grafted by magnetic nanoparticles for oil separation from emulsified oil wastewaters. *Chemical Engineering Journal* **2018**, *337*, 10-18, doi:10.1016/j.cej.2017.12.084.
11. Lu, T.; Zhang, S.; Qi, D.; Zhang, D.; Zhao, H. Enhanced demulsification from aqueous media by using magnetic chitosan-based flocculant. *J Colloid Interface Sci* **2018**, *518*, 76-83, doi:10.1016/j.jcis.2018.02.024.
12. Liang, J.; Li, H.; Yan, J.; Hou, W.J.E.; Fuels. Demulsification of Oleic-Acid-Coated Magnetite Nanoparticles for Cyclohexane-in-Water Nanoemulsions. **2014**, *28*, 6172-6178, doi:10.1021/ef501169m.
13. Liang, J.; Du, N.; Song, S.; Hou, W. Magnetic demulsification of diluted crude oil-in-water nanoemulsions using oleic acid-coated magnetite nanoparticles. *Colloids and Surfaces A: Physicochemical and Engineering Aspects* **2015**, *466*, 197-202, doi:10.1016/j.colsurfa.2014.11.050.